ELSEVIER

Physica D 89 (1995) 169–183

PHYSICA D

# Waves and synchrony in networks of oscillators of relaxation and non-relaxation type

David Somers [a,1], Nancy Kopell [b,2]

[a] *Department of Brain and Cognitive Sciences, Massachusetts Institute of Technology, E25-618, 45 Carleton Street, Cambridge, MA 02139, USA*

[b] *Department of Cognitive and Neural Systems, Department of Mathematics, Boston University, 111 Cummington Street, Boston, MA 02215, USA*

Received 4 August 1994; revised 30 January 1995; accepted 3 May 1995
Communicated by C.K.R.T. Jones

**Abstract**

Arrays of relaxation oscillators behave differently in the presence of a non-uniformity of natural frequencies and/or coupling inputs than do arrays of phase oscillators coupled through phase differences. Phase oscillators compensate for non-uniformities by creating phase differences among the oscillators; relaxation oscillators coupled via "fast threshold modulation" (FTM) can respond by changing wave forms while leaving the fast jumps synchronous. For arrays of relaxation oscillators including chains, this allows synchrony to be a solution, even though the oscillators have different amounts of inputs from other oscillators; for phase-difference coupled oscillators in a chain, the generic solution is a travelling wave. Relaxation oscillators coupled through FTM also allow the encoding of patterns of oscillators into domains in which oscillators are in synchrony, with different domains in antiphase.

## 1. Introduction

This paper is concerned with some contrasting behavior of interacting relaxation oscillators versus non-relaxation oscillators. In a previous paper [1] we showed that a ring of identical relaxation oscillators, coupled locally in a manner that mimics fast excitatory synapses, can lead to synchronization within a couple of cycles, while non-relaxation oscillators, with the same coupling, synchronized much more slowly. Here we analyze how relaxation and non-relaxation oscillators compensate for differences in natural frequency between the interacting oscillators and/or for differences in amounts of coupling input. We also show that the distinction between the compensatory mechanism used by interacting relaxation oscillators and that used by interacting phase oscillators has implications for the behavior of networks of oscillators with uniform natural frequency as well as for the behavior of networks with varying frequency.

We start in Section 2 by considering pairs of oscillators. It is easy to show that phase oscillators that interact via the differences in their phases can phase-lock if the differences in their natural frequencies are not too large. The phase difference in a stable locked

[1] Supported in part by NASA (NGT-50497) and the McDonnell-Pew Center for Cognitive Neuroscience at MIT.
E-mail: somers@ai.mit.edu.
[2] Supported in part by NSF (DMS-8901913), NIMH-47150.
E-mail: nk@math.bu.edu.


*SSDI* 0167-2789(95)00198-0

solution increases with the difference in the natural frequency [2,3]. This is also true of any more general oscillators and interactions that can be shown to behave like such phase oscillators, e.g., when the coupling is weak [4]. We consider the contrasting case of a pair of relaxation oscillators. Following the analysis of [1], we utilize a relaxation oscillator coupling form that we named "fast threshold modulation" or FTM. Generalizing a result of [1] for identical oscillators, we prove that for relaxation oscillators having close enough frequencies and waveforms, a pair of oscillators compensates for differences between the oscillators by changing the waveform of the locked output, while keeping the fast jumps *synchronous*. Computer simulations demonstrate this synchronous behavior for oscillators whose natural frequencies differ by as much as 50%.

For relaxation oscillators, but not phase oscillators, the argument generalizes to arrays of many oscillators. A key idea in the analysis is to consider as the central objects not the isolated oscillators, but the trajectories the oscillators would follow if all jumps in the network were synchronous. We use this in Section 2 to prove that if oscillators in the network are similar to one another, and they have a similar amount of coupling input, then (under a technical condition which holds for large classes of relaxation oscillators), the network has a stable solution, which in the relaxation limit, has synchronous jumps.

The distinction between the compensatory mechanisms (creating a phase difference in one case, and altering waveform in the other) creates contrasting behavior of *chains* of phase oscillators versus relaxation oscillators, even if the oscillators in the chain are identical. As shown in [5], chains of *phase* oscillators that phase-lock generically produce travelling waves. The waves were shown in [5] to be a consequence of boundary effects: the oscillators at the ends receive different input than those in the middle, and compensate for the difference by setting up phase differences all along the chain. These phase differences are independent of the coupling strength.

In Section 3 we show that chains of equal relaxation oscillators, coupled via FTM, can compensate for differences of inputs at the boundaries by changes of waveform that remain localized in oscillators near the boundaries. Hence, in the relaxation limit, the fast jumps are synchronous across the chain. Because the end oscillators have half the input of the middle ones, this does not follow directly from the work of Section 2. However, we can give conditions under which synchrony is the $\epsilon \mapsto 0$ limit for the solutions. (The work in [1] also produced synchrony for an array of relaxation oscillators. However, in [1] the array was a *ring*, so there were no boundary conditions to produce phase differences. In that paper, the emphasis was not on the phase relationships (since synchrony was expected), but on the *speed* of locking.)

If the oscillators are not at the relaxation limit, or the coupling is weak, the oscillators are not synchronous. In Section 3 we also discuss transitions in chains between phase-oscillator like behavior and relaxation-oscillator like behavior. In particular, we present simulations to demonstrate how stimuli that change the effective strength of coupling can switch the system from wave behavior to near synchrony.

Section 4 is devoted to chains in which the oscillators are not all identical. Section 4.1 deals with chains whose end oscillators have different properties from the interior ones, and shows that synchrony can be maintained within a chain of relaxation oscillators if the end oscillators are not too different. Section 4.2 discusses the more general case of unequal oscillators, including a gradient of frequency along a chain. As in Section 3, we present simulations to show that relaxation oscillators behave differently from phase oscillators, and we explain why.

The contrasting behavior of chains of relaxation and phase oscillators has further consequences for arrays of oscillators, as we show in Section 5. In that section, we shall be concerned with the situation in which *pairs* of oscillators are capable of stable in-phase and antiphase locking. It is easy to construct phase oscillators for which this is true [6–8]. Relaxation oscillators have also been shown to be capable of bistability [9–12]. In Ref. [9] we showed that, with excitatory FTM coupling, pairs of oscillators can have stable in-phase and antiphase solutions, providing that the times to traverse the left-hand and right-hand branches of the relaxation oscillators are sufficiently distinct.

In Section 5 we demonstrate and analyze the phenomena of "fractured synchrony" in one-dimensional arrays (e.g. rings) of relaxation oscillators pairwise capable of bistability, and "fractured waves" in arrays of phase oscillators pairwise capable of bistability. By fractured synchrony we mean that some contiguous set (or domain) of oscillators are in synchrony, but roughly in antiphase with neighboring domains. We explain why this is possible for arrays coupled by FTM, but not (generically) for arrays of phase oscillators, in which the behavior on each domain is that of a travelling wave.

## 2. Pairs of oscillators

A pair of oscillators interacting through phase differences satisfies equations of the form

$$\theta_1' = \omega_1 + H_1(\theta_2 - \theta_1)\,, \tag{1}$$

$$\theta_2' = \omega_2 + H_2(\theta_1 - \theta_2)\,. \tag{2}$$

Here $\theta_i$ are the phases of the oscillators, $\omega_i$ are the frequencies of the uncoupled oscillators, and $H_i$ are smooth $2\pi$-periodic functions of the phase differences. Let $\phi \equiv \theta_2 - \theta_1$. Then (1), (2) may be reformulated as

$$\begin{aligned}\phi' &= \omega_2 - \omega_1 + H_2(-\phi) - H_1(\phi) \\ &\equiv \delta - H(\phi)\,,\end{aligned} \tag{3}$$

where $\delta$ is the difference in frequency. If $H_1 = H_2$, then $H$ equals twice the odd part of $H_i$ so $H(0) = 0$, and hence synchrony ($\phi = 0$) is a solution if $\delta = 0$. We assume that $H' > 0$ for $\phi$ in a neighborhood of $\phi = 0$, so the synchronous solution is stable. For $\delta \neq 0$ but not too large, and $H_1 = H_2$, $\delta - H(\phi)$ may be solved for a stable critical point of $\phi$. The greater the frequency difference (within this range), the greater the resulting phase difference between the oscillators; for small $\delta$, the relationship between $\phi$ and $\delta$ is close to linear. Similarly, differences between $H_1$ and $H_2$, if not too large can be compensated by a non-zero phase lag.

We now contrast this with a pair of relaxation oscillators, coupled by "fast threshold modulation". Each

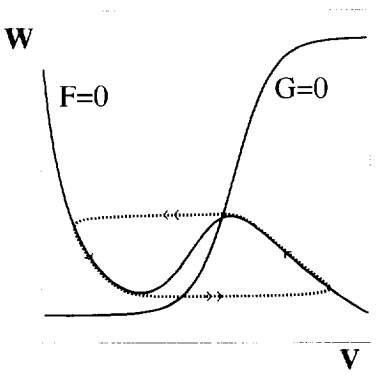


Fig. 1. Nullclines and phase plane trajectory (dashed) for a single relaxation oscillator (Morris–Lecar, see Appendix). When the relaxation parameter, $\epsilon$, is small the trajectory slowly traverses the outer branches of the cubic-shaped nullcline toward the local extremum of each branch. When an extremum is reached, the trajectory jumps rapidly to the other branch.

of the uncoupled oscillators is defined by a pair of equations of the form

$$\epsilon v_i' = F_i(v_i, w_i)\,, \tag{4}$$

$$w_i' = G_i(v_i, w_i)\,. \tag{5}$$

Here $0 < \epsilon \ll 1$, and (4), (5) is assumed to have a stable limit cycle. The nullcline $F(x, y) = 0$ is assumed to be cubic shaped, as in the van der Pol oscillator and other equations associated with descriptions of neurons and collections of neurons. (See Fig. 1). As in [1], the coupling we shall use changes (4) to

$$\epsilon v_i' = F_i(v_i, w_i, I(v_j))\,, \tag{6}$$

where $v_j$ denotes the $v$-variable of the other oscillator, and $I(v_j)$ is the coupling signal. We assume that $I(v_j)$ is a saturating sigmoidal, as in Fig. 2a. Furthermore, we assume that increasing $I$ has the effect of raising the nullcline $F_i(v, w, I) = 0$, as in Fig. 2b. This increase in $I$ corresponds to excitatory input of the neural oscillators, either in single-neuron conductance-based models such as Hodgkin–Huxley [13] or Morris–Lecar [14] or ensemble descriptions such as Ellias–Grossberg [15] or Wilson–Cowan [16]. Finally, we assume that for all values of $I$ in the range of $I(v)$, the outer branches of the "cubic" $F_i(v, w, I) = 0$ lie in the saturated portions of $I(v)$, so $I(v)$ is independent of $v$ on each branch. In the relaxation limit, such

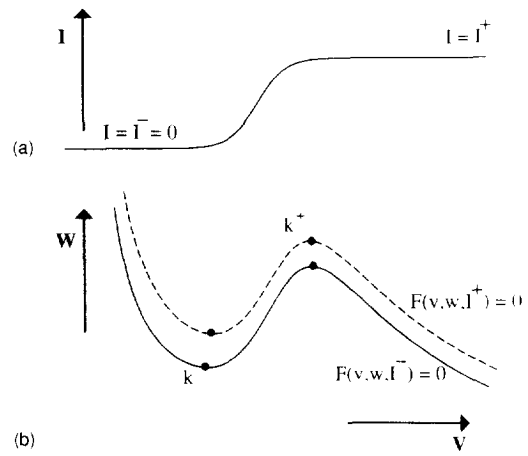


Fig. 2. Heaviside coupling. (a) shows a sigmoidal coupling function, $I(V)$, for which the non-constant ranges of the function lie in the middle branch of the cubic nullcline (shown in (b)). Since the phase-plane trajectory hugs the outer branches and rapidly jumps between these branches, the coupling function assumes one of two constant values, $I^-$ or $I^+$, determined by the branch on which the input oscillator lies. $I^-$ and $I^+$ define different cubic nullclines with the $I^+$ nullcline shifted upward, possibly with a change of shape as shown in (b). The trajectory of a coupled pair of identical oscillators can be described by these two cubics and the rapid transitions between them. The local extrema or "knees" are important transition points.

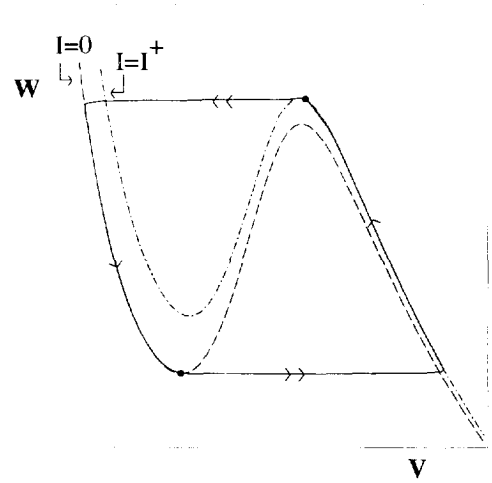


Fig. 3. The limit cycle with input (LCI) for an oscillator is defined by pieces of the left branch of the $I = 0$ cubic and the right branch of the $I = I^+$ cubic. The LCI represents the trajectory followed by an oscillator when its onsets and offsets are synchronous with those of the oscillators that provide its input.

a system behaves the same as one in which $I(v)$ is a step function, with the discontinuity in the middle branch of each cubic (see Fig. 2b).

In the treatment we shall give, the primary objects are not the uncoupled oscillators, but the oscillators as changed by their inputs. We define the LCI (limit cycle with input) as the cycle that would be followed by the oscillator providing that the input jumps at the same time as the jumps of the oscillator (See Fig. 3). If the oscillators are the same and the coupling is symmetric, the LCI reduces to what was called the LSS (limiting synchronous solution) in [1]. In the more general case, the two oscillators can have different associated LCI's. We shall show that if the LCI's associated with the two oscillators are not too different, and an analogue of the "compression hypothesis" of [1] holds, then there is indeed a periodic solution in which the jumps of the two oscillators are simultaneous. This will show that the relaxation oscillators, interacting through fast threshold modulation, compensate for differences by changes in waveform, rather than by phase lags.

To state and prove the result, we need some further definitions. We define the *size* of an interval $J$ on one of the cubic-like nullclines to be the time necessary to traverse this interval, and denote it by $|J|$. For each oscillator, $i$, we denote the lower and upper knees (extrema) of their LCI's as $k_i$ and $k_i^+$, respectively. Let $j(k_i)$ and $j(k_i^+)$ represent the points on the opposite branches reached on a jump from the respective knees. We define $\overline{L_i}$ as the part of the left branch of the LCI between $j(k_i^+)$ and $k_i$ and similarly define $\overline{R_i}$ on the right branch between $j(k_i)$ and $k_i^+$. (See Fig. 4.) Let $L_i$ denote the part of the left-hand branch of the lower nullcline of oscillator $i$ that is below the lower knee of the upper nullcline. Define $R_i$ in a similar manner, as in Fig. 4. Note that for a fixed $I$ the $L_i$ and $R_i$ are defined uniquely. For $J$, any subinterval of $L_i$ or $R_i$, let $j(J)$ denote the image after a rightward or leftward jump. We shall require

*Hypothesis C.* For any interval $J$ as above, $|j(J)| < |J|$.

This hypothesis was called the "compression hypothesis" in [1]. Hypothesis C is closely related to the central condition needed for stability of the in-phase

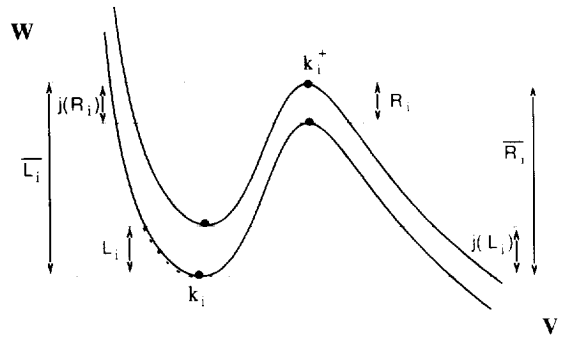


Fig. 4. The knees of the $I^-$ and $I^+$ cubics define intervals relevant to synchronous jump behavior. $\overline{L_i}$ and $L_i$ are defined as the pieces of the left branch of the $I^-$ cubic which lie below the upper and lower knees, respectively, of the $I^+$ cubic. All jumps from the right branches map into $\overline{L_i}$. $L_i$ is the subset of $\overline{L_i}$ in which a trailing oscillator will jump synchronously with a leading oscillator to the right branch. $j(L_i)$ describes the interval into which trajectories in $L_i$ will jump. The intervals $\overline{R_i}$, $R_i$, and $j(R_i)$ are defined analogously.


Fig. 5. Slow variable time course for the Morris–Lecar oscillator. The time required to traverse a $w$ interval increases as threshold (a "knee") is approached. This "scalloped" shape of the time course ($w' \cdot w'' < 0$) satisfies Hypothesis C.

solution. It holds whenever the time course of $w(t)$ in the synchronized solution has a shape as in Fig. 5. (This shape was referred to as "scalloped" in [1,9].) The ratio of the slopes of $w$ just before to just after a local maximum or minimum is a measure of the compression. (See Ref. [1] for more details.)

We shall also require that the LCI's be sufficiently close to each other. We can compare the equations on the two LCI's by normalizing each slow branch to take unit time to traverse. By "close" we shall mean that the normalizing constants are close, and that the resulting normalized vector fields are $C^1$ close on each branch. We will prove

*Theorem 2.1.* Suppose Hypothesis C holds and the LCI's of the two oscillators are sufficiently close. Then there is a periodic solution for the coupled system such that the rightward (respectively, leftward) jumps of each oscillator *synchronize* with the rightward (respectively, leftward) jumps of the other. This solution is stable and locally unique.

This generalizes a result we proved for *identical* oscillators [1]. For the rest of this paper we need a still more general result, valid for networks, which we now formulate. Consider a network of relaxation oscillators with any "non-disjoint" set of interconnections, coupled via FTM. (By "non-disjoint" we simply mean that every oscillator is connected at least indirectly to every other oscillator.) As for a pair of oscillators, we define the LCI for each oscillator of the network to be the trajectory that would be followed (in the $\epsilon \to 0$ limit) provided that all oscillators in the network jump in a given direction at the same time. (If the network is synchronized, this is the orbit that must be followed.) As for the pair, we assume that the input from any oscillator (in the $\epsilon \to 0$ limit) depends only on whether that oscillator is "on" or "off." Then the following generalizes Theorem 2.1:

*Theorem 2.2.* Suppose Hypothesis C holds for each LCI in the network. Then if the LCI's are sufficiently close, there is a periodic solution for the coupled system such that the jumps in either direction synchronize with the jumps in that direction for all oscillators in the network.

*Remark.* For a network of identical oscillators, each with an identical number and strength of inputs (not necessarily small) from the other network elements, the LCI's are identical. The closeness hypothesis on the LCI's continues to hold under O(1) perturbations of the oscillators and the coupling. Thus synchrony is possible even if the number of connections or the strengths of connections to each element vary across the population. This contrasts with the behavior of other networks of oscillators, in which connection weights between oscillators must be normalized to achieve synchrony [17].

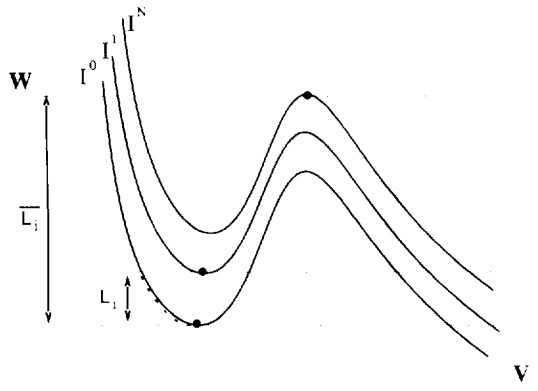


Fig. 6. Defining the domain of the Poincaré map in higher dimensional networks. Relaxation oscillators that receive multiple inputs have trajectories that are defined by several cubic nullclines, each determined by the number and size of synaptic inputs received. The change of a single input may still cause an early jump. The knees of the uppermost cubic ($I^N$) and lower two cubics ($I^0$ and $I^1$) define the intervals $L_i$ and $\overline{L_i}$ as in Fig. 4. The set of $n$-dimensional points for which each oscillator lies in its $L_i$ and at least one oscillator lies at its lower knee, defines the domain of the map $\mathcal{P}_L$.

*Proof of Theorem 2.2.* We shall construct a Poincaré map whose fixed points will correspond to the required orbit. The domain of the map is the points at which at least one oscillator is at its lower knee. More specifically, let $\overline{L}_i$ be defined as before for two oscillators, with the upper cubic given by the natural dynamics plus *all* the inputs. $L_i \subset \overline{L}_i$ is the portion of $\overline{L}_i$ below the cubic corresponding to *one* input. See Fig. 6. Let

$$L = \bigcup_{j=1}^{n} L_1 \times L_2 \times \ldots \times \{k_j\} \times \ldots \times L_n ,$$

$$\overline{L} = \bigcup_{j=1}^{n} \overline{L}_1 \times \overline{L}_2 \times \ldots \times \{k_j\} \times \ldots \times \overline{L}_n .$$

$L$ represents these $n$-tuples of points for which all oscillators will make simultaneous right jumps in the next instant (in the limit $\epsilon \to 0$). $\overline{L}$ are those points for which at least one oscillator will jump immediately. $R$ and $\overline{R}$ are defined analogously, using $\{k_j^+\}$ instead of $\{k_j\}$. $L, \overline{L}, R$ or $\overline{R}$ may be visualized as the neighborhood of a corner of an $n$-dimensional cube. For $n = 2$, see Fig. 7.

In the $\epsilon \mapsto 0$ limit, the synchronous jumps and subsequent flows along a branch provide natural maps

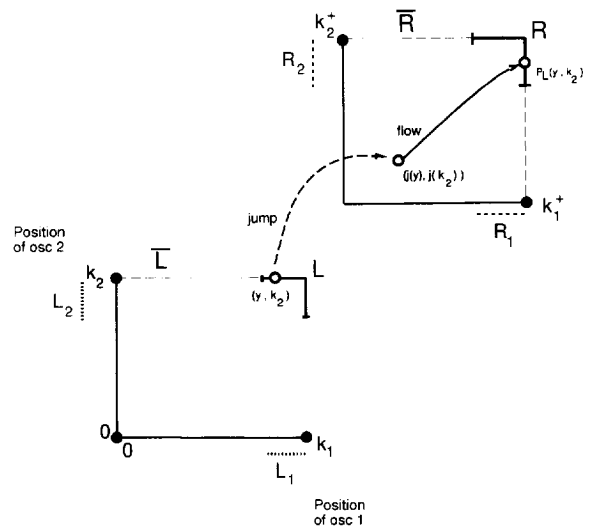


Fig. 7. One half of the Poincaré map for a pair of coupled oscillators. $L$ and $R$ (solid line corners) represent the sets of points for which both oscillators make simultaneous jumps in the next instant. $\overline{L}$ and $\overline{R}$ (dashed line corners) define the supersets of $L$ and $R$ for which at least one oscillator is at the jump threshold. After a synchronous jump from $L$ (or $R$), oscillators then flow until they lie in $\overline{R}$ (or $\overline{L}$). A synchronous jump and the subsequent flow therefore describe a map from $L$ to $\overline{R}$ (or from $R$ to $\overline{L}$.) The intervals $R_i$ and $L_i$ are as in Fig. 2.

$\mathcal{P}_R: R \to \overline{L}$ and $\mathcal{P}_L: L \to \overline{R}$. To define $\mathcal{P}_R$ on $R$, we consider separately each "face" $R_1 \times R_2 \times \ldots \times \{k_j^+\} \times \ldots \times R_n$. For each point in that face, the image after the jump is a point on the product of the left-hand branches of the LCI's. (This requires that the interconnections be "non-disjoint", so that all sufficiently close oscillators jump at the same time.) The flows on the left-hand branches then take that point to a point of $\overline{L}$, the first point at which one of the $n$ components is at the lower knee of the lower branch. We define the latter point to be the image under $\mathcal{P}_R$. The map $\mathcal{P}_R$ is defined analogously for the other faces, and similarly for $\mathcal{P}_L$.

We wish to consider $\mathcal{P}_L \circ \mathcal{P}_R$, to look for a fixed point. To do this, we must have the image of $\mathcal{P}_R$ in the domain of $\mathcal{P}_L$. Thus, we restrict the domain of $\mathcal{P}_R$ to $\hat{R} = \mathcal{P}_R^{-1}(L) \cap R$.

We first assume that all LCI are identical. Then $\{k_1^+\} \times \ldots \times \{k_n^+\}$ is a fixed point of $\mathcal{P}_L \circ \mathcal{P}_R$. Note that each face of $\hat{R}$ is mapped onto itself under $\mathcal{P}_L \circ \mathcal{P}_R$. (This is true because edges of a face correspond to

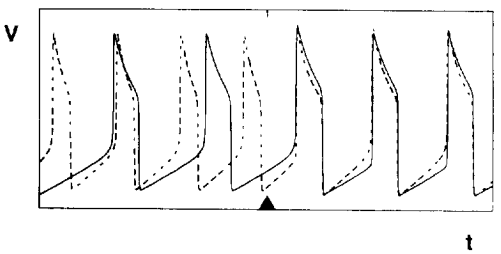


Fig. 8. Two uncoupled relaxation oscillators, with natural frequencies that differ by 50% ($\epsilon = 0.01, \epsilon = 0.015$), synchronize their onset and offset times once coupling is activated between the oscillators ($\alpha = 0.2$; triangle marks coupling onset). The frequency differences are compensated for by modifications of the oscillators' waveforms. Note the change in amplitude and pulse duration with coupling onset.

points for which two oscillators are at their upper knee $k^+$, and this is preserved under $\mathcal{P}_L \circ \mathcal{P}_R$ if all LCI are identical.) Using as coordinates for the face the Cartesian product of the coordinates for each LCI, it follows from Hypothesis C that $\mathcal{P}_L \circ \mathcal{P}_R$ is a contraction map on each face, and hence on $\hat{R}$. The conclusion of the theorem now follows by noting that a perturbation of a contraction map is also a contraction map, and therefore has a unique fixed point in the domain of the map. □

*Remark.* A related theorem was proved by Pinsky [18] using different methods. The result in [18] provides approximate (and, possibly exact) synchronous solutions for a network of somewhat different relaxation oscillators.

The ability of FTM-coupled relaxation oscillators to compensate for differences in their natural frequency is demonstrated in Fig. 8. The onset of FTM coupling rapidly synchronizes a pair of oscillators that have a 50% difference in their natural frequencies. FTM coupling achieves synchronization by modifying the oscillator waveform.

## 3. Boundary effects in chains of identical oscillators

### 3.1. Waves and synchrony

We first review some results in [5] concerning chains of phase oscillators, and then contrast those results with the behavior of chains of relaxation oscillators. It was shown in [5] that the behavior of chains of $N$ phase oscillators can be analyzed using a "thermodynamic" limit, in which the length of a chain grows without bound but the interactions between neighboring oscillators remains fixed. The analysis in [5] was done without assuming that the coupling in the two directions is the same. The equation for the $j$th oscillator ($j \neq 1, N$) is then

$$\theta_j' = \omega_j + H^+(\theta_{j+1} - \theta_j) + H^-(\theta_{j-1} - \theta_j), \qquad (7)$$

where $H^+$ and $H^-$ are $2\pi$-periodic functions representing coupling in the two-directions. For $j = 1, N$, one of the two coupling terms is absent. Using the limiting equations, it was shown that the generic behavior for a chain of identical oscillators ($w_j \equiv w$) is a travelling wave in which the phase lag $\phi_j \equiv \theta_{j+1} - \theta_j$ is essentially constant (except for a boundary layer). This constant phase lag is either $\phi_L$ or $\phi_R$, where $\phi_L$ and $\phi_R$ are defined by $H^-(-\phi_L) = 0$, $H^+(\phi_R) = 0$, with each function having a positive slope at the relevant zero. There is a formula [19] that can be used to determine whether the lag is $\phi_L$ or $\phi_R$. The case $H^+ = H^- \equiv H$ is non-generic; with this symmetry and large $N$, the oscillators display phase lags with $\phi_j \approx \phi_L$ for the left half of the chain, $\phi_j \approx \phi_R$ for the right half of the chain with a "boundary layer" in between. For smaller values of $N$, the boundary layer comprises a larger subset of the chain, so the lags do not appear so constant.

In contrast to chains of (generic) phase oscillators, chains of equal relaxation oscillators, coupled through Fast Threshold Modulation, can (in the limit as $\epsilon \mapsto 0$) *synchronize* their jumps. In a prior paper [1] we proved that synchrony is stable for rings (no boundary) of identical relaxation oscillators coupled through FTM. Here we show that the differences in input to the oscillators at the ends of the chain versus the os-

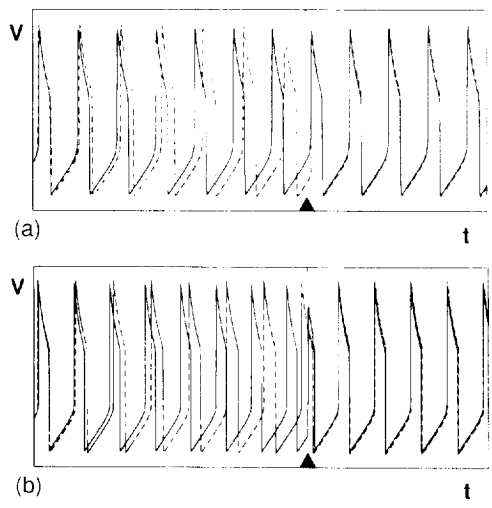


Fig. 9. Synchronization of chains of relaxation oscillators occurs rapidly despite the lower input to the end oscillators of the chain. (a) A "chain" of three Morris–Lecar oscillators ($\epsilon = 0.01$, $\alpha = 0.1$), in which the middle oscillator receives coupling input from its two neighbors and the end oscillators receive only one coupling input. This input difference produces different LCI and different periods for the middle and end oscillators. This difference is demonstrated by starting the oscillators with identical initial conditions and switching the coupling to LCI mode (inputs from self, rather than neighbors). The two end oscillators have the same LCI and thus remain synchronized (traces overlaid), while the middle oscillator drifts. At the mark, LCI coupling is replaced by chain coupling. The relaxation oscillators compensate for differences in input to the end oscillators and the chain synchronizes within a single jump. (b) same as (a) but chain contains 40 oscillators ($\epsilon = 0.001$). Time course of end oscillators (1,40) and three middle oscillators (2,3,20) are shown. In LCI mode the ends and middle drift apart, but rapidly synchronize when chain coupling is activated.

cillators in the middle need not create waves. This is demonstrated in Fig. 9 for Morris–Lecar oscillators [14] (see Appendix for equations). The compensatory mechanism is essentially the same as for a pair of oscillators with different frequencies or different coupling inputs (i.e. with different LCI's). Here the LCI's for the middle oscillators of the chain are the limit cycles associated with inputs from two other oscillators (See Fig. 10a) and the LCI's for the end oscillators are the limit cycles with input from one other oscillator (See Fig. 10b).

The result for chains does not automatically follow from Theorem 2.2 because the difference in inputs to the end oscillator and the middle ones may not be "sufficiently small". However, in the case of chains, the necessary condition for synchrony can be formulated directly by comparing the LCI of the end oscillators with those of the interior ones.

If $I^- = 0$, there are two cases that yield synchrony; the cases differ in the relative time the middle and end oscillators require to traverse the right branches of their LCI's. Note that the left branch of the LCI for end oscillators is a subset of that for middle oscillators, and so the middle oscillators must take longer to traverse the left branches of their LCI's. Consider the case in which the middle oscillators also take longer to traverse the right branch of their LCI's. For synchrony, it is sufficient that there be points $q_L$, $q_R$ on the LCI of the middle oscillators, as in Fig. 10c, for which the time from $j(q_L)$ to $q_R$ and the time from $j(q_R)$ to $q_L$ are the same as the times along the slow pieces in the LCI of Fig. 10b. The point $q_L$ (resp. $q_R$) should lie below (resp. above) the lower (resp. upper) knee of the middle nullcline, as in Fig. 10c, so the change of a single input causes a jump. Now consider trajectories in which the middle oscillators traverse from $j(q_L)$ to their $k^-$ in a time, $\tau$, *less* than the end oscillators require to traverse from $j(k)$ to their $k^+$. In this case, synchrony requires that there be a point $\widehat{q_R}$ above the upper knee of the lower nullcline (see Fig. 10d) such that the end oscillators traverse from $j(k)$ to $\widehat{q_R}$ in time $\tau$.

These mechanisms generalize to the situation in which middle and end oscillators have distinct LCI left (as well as right) branches. Thus, the oscillators may exhibit chain synchronization over a wide range of parameters. The ability to compensate for differences in LCI branch times increases with coupling strength.

### 3.2. *Transitions*

The two behaviors described above (waves and synchrony) can occur in different parameter regimes of the same equations. There are two natural parameters that provide the transitions between these regimes. We first discuss those parameters and how they change the behavior of the chain. We then show how changes in excitatory input to the oscillators can effectively change one of those parameters to move the system

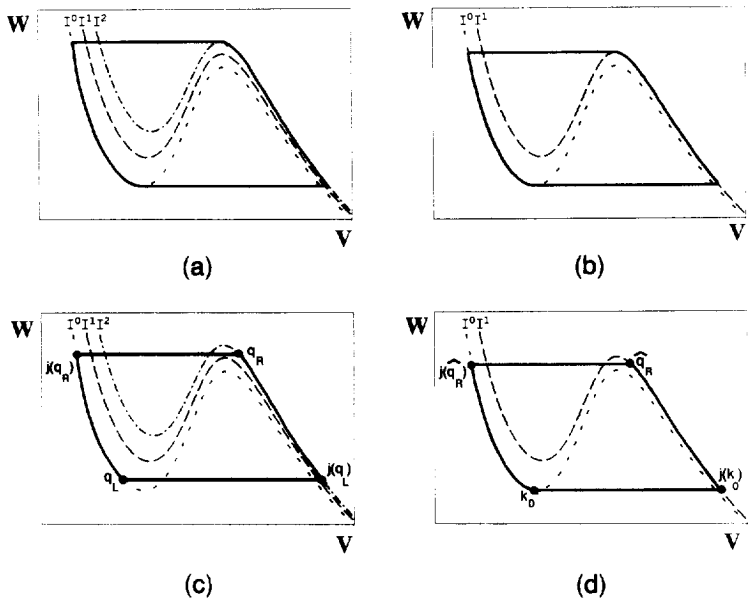


Fig. 10. Compensation mechanisms in chain synchronization. (a) Relaxation oscillators in the middle of a nearest neighbor chain receive 2 coupling inputs and thus their LCI are determined by the nullclines ($I^0$, $I^1$, $I^2$) with 0, 1, and 2 coupling inputs of size $I^+$. (b) The two end oscillators receive only one input, thus even for chains of identical oscillators, the end oscillators have different LCI than the middle oscillators. (c) An oscillator with longer LCI times (shown here for the middle oscillators) can jump synchronously with the faster (end) neighbor provided that points $q_L$, lying below the lower knee of the $I^1$ cubic, and $q_R$, lying above the upper knee of the $I^1$ cubic exist such that the time from $j(q_L)$ to $q_R$ and the time from $j(q_R)$ to $q_L$ are the same as the times along the LCI of the faster (end) oscillator (shown in (b)). (d) FTM Coupling can also compensate when each oscillator has a longer LCI time only for one branch. For instance, if the middle oscillator is slower on left branch as in (c), but the end oscillator is slower on the right, synchrony requires that there be a point $\widehat{q_R}$ above the upper knee of the $I^0$ cubic, such that the end oscillators traverse from $j(k_0)$ to $\widehat{q_R}$ in the time the middle oscillators traverse from $j(q_L)$ to $k^+$.

between the two regimes.

One of the two parameters is $\epsilon$, the ratio of the two time scales. As discussed above, in the limit as $\epsilon \mapsto 0$, there can be a solution in which the (instantaneous) transitions occur synchronously along the chain, in spite of edge effects. For $0 \ll \epsilon \ll 1$, there is an $o(1)$ delay between the transition of one oscillator and that of the next. For $\epsilon = O(1)$, the oscillators are not in the relaxation regime, and they cease to interact via the FTM mechanism. The simulations of Fig. 11 show that for $\epsilon \gg 0$ there are waves, and for $\epsilon$ smaller, the wave speed increases. (Compare this to Fig. 9.) Thus neuromodulators that effectively increase the difference between the active time scales of neural relaxation oscillators (e.g. Ref. [20]) may decrease the delays (relative to the period) between successive oscillators in a chain.

The other relevant parameter is the effective strength of coupling. For any set of limit cycle oscillators, if the coupling is sufficiently weak, then the interactions of the oscillators are, to lowest order in the coupling, through their phase differences [4]. This is true even of relaxation oscillators, with $\epsilon$ near zero; however, the coupling must then be very weak, i.e. less than $O(\epsilon)$. For relaxation oscillators with coupling of the form described in Section 2, as the coupling increases from very weak to medium, the interactions change from phase difference interactions to FTM interactions.

The effective strength of coupling may be changed without actually changing the maximal conductance of the synapse. Any modulation that changes the shape of the gating function can also change the effective strength of coupling. In particular, if the gating function changes from being a shallow sigmoid to a much steeper one (e.g. Refs. [21,22]), the total synaptic current over a cycle can increase significantly (even if

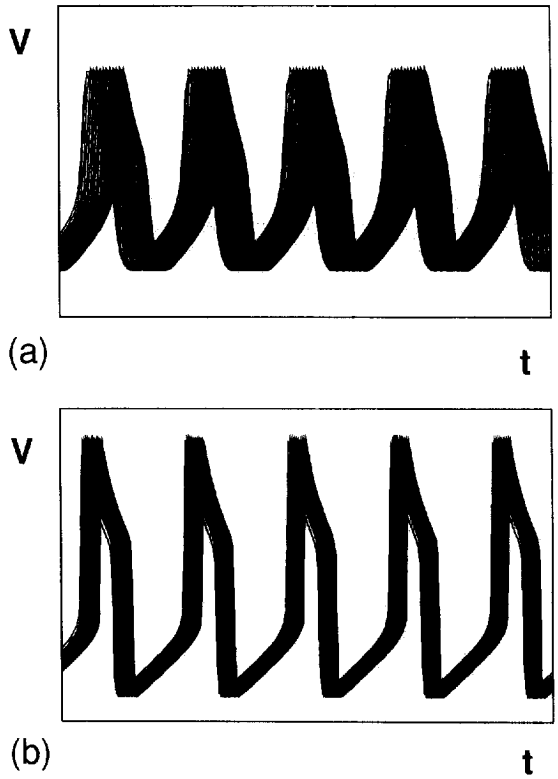


Fig. 11. Asymptotic travelling wave behavior for chains away from the relaxation limit. Chains of 40 oscillators ($\alpha = 0.1$) were started with synchronous initial conditions, but with $\epsilon \gg 0$ the edge effects of coupling led to travelling waves (shown after 200 cycles, with all 40 traces overlaid). (a) $\epsilon = 0.25$; (b) $\epsilon = 0.02$. As $\epsilon$ approaches zero the wave speed (relative to the period) increases and the dispersion or total lag of the travelling wave decreases. See Fig 9b for synchrony with $\epsilon = 0.001$.

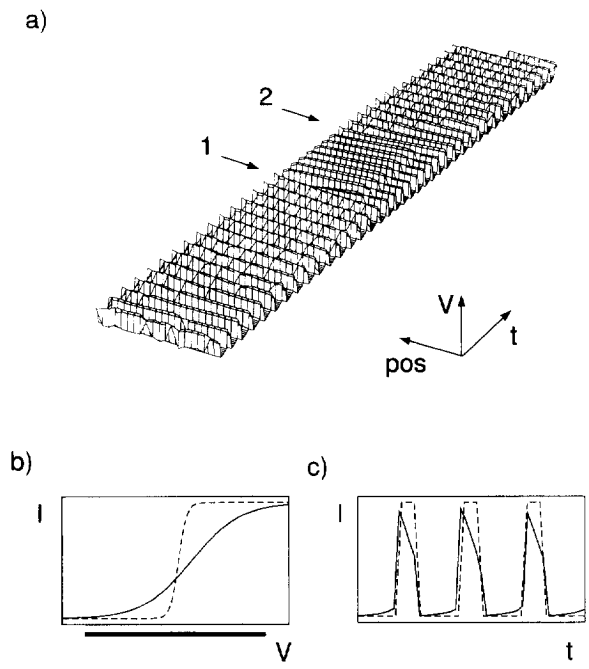


Fig. 12. Input driven modulation of slope of synaptic coupling function can shift relaxation oscillators between FTM and non-FTM behavior. A chain of 20 identical relaxation oscillators ($\epsilon = 0.01$) coupled in one direction (left to right, $\alpha = 0.5$) with a ramp coupling function (shown as solid line in (b),(c); $v_6 = 0.10$, $v_7 = 0.30$) develops a leftward moving travelling wave due to the "defect" in input to the left end of the chain. (Two way coupling yields two oppositely directed waves, each propagating outward from the middle.) At 1, the coupling function is modulated to a Heaviside step (shown as dashed line in b,c; $v_6 = 0.017$, $v_7 = 0.05$) without changing the maximal synaptic conductance. The network rapidly synchronizes. At 2, coupling switches back to the ramp function, and travelling waves slowly re-emerge. (b) Synaptic coupling functions. Dark bar represents voltage range of inputs. (c) Time course of synaptic input.

the maximal conductance does not change). The effect on the network is illustrated in Fig. 12.

*Remark.* More can be said about the effects of changing the shape of the gating function. When $\epsilon > 0$, the sigmoidal coupling function (see Fig. 2) no longer behaves like a "Heaviside" step. Since coupling input increases during the (non-instantaneous) jump of the leading oscillator, there is a transition period during which the nullcline is shifting and the trailing oscillator is not yet at threshold. This nullcline shift may slow down the trailing oscillator, as described in [9], and induce a substantially longer phase lag than that due to $\epsilon \neq 0$ alone. Increasing the coupling strength decreases the transition time to threshold and thus decreases the phase lag. Alternatively, replacing the sigmoid ramp with a Heaviside step will eliminate the phase lags due to the shifting nullcline and thus can also move the network to synchrony, as in Fig. 12.

## 4. Chains of oscillators having variation in frequency

In the previous section, we discussed chains of identical oscillators, and the contrast in behavior between phase oscillators and relaxation oscillators coupled with FTM. In this section we allow the oscillators to

have different frequencies and again contrast the two cases.

### 4.1. Changes in end oscillators only

One important situation concerns chains in which all the oscillators are identical except for the end oscillators. In both phase and relaxation oscillator cases, the change of the end oscillators acts like a change of boundary conditions. For the relaxation case, it follows immediately from the methods of Section 3 that a small enough change still allows synchrony of the jumps in the $\epsilon \mapsto 0$ limit. For phase oscillators, we now show that a change of the end oscillators changes the phase relationships within the travelling wave.

We start with the phase oscillators, as described by (7). To understand how changing $w_j$ at one or both ends of the chain affects the phase lags, $\phi_j$, of the stable solution, we must go deeper into the analysis done in [5]. The time-independent solution for the $\phi_j$ was shown in [5] to converge for large $N$, in some appropriate sense, to that of the continuum equation

$$0 = \omega(x) + 2f(\phi)_x + \frac{1}{N} g(\phi)_{xx}, \tag{8}$$

subject to the boundary conditions

$$H^-(-\phi) = 0 \text{ at } x = 0, \quad H^+(\phi) = 0 \text{ at } x = 1. \tag{9}$$

These boundary conditions encode the difference between the equations $j = 1, N$ and the other equations. Here $0 \le x \le 1$, $2f(\phi) \equiv H^+(\phi) + H^-(\phi)$, $2g(\phi) \equiv H^+(\phi) - H^-(\phi)$, and $\phi(j/N) \approx \phi_j$.

If $\omega_j \equiv \omega$, then the continuum limit analogue uses $\omega(x) \equiv \omega$, a constant function. If $w_j \equiv \omega$ except for $j = 1, N$, the relevant continuum limit formulation uses the same $\omega(x)$, but has different boundary conditions. If $\omega_1 - \omega_j \equiv \Delta_1$ and $\omega_N - \omega_j \equiv \Delta_N$, the boundary conditions $H^-(-\phi) = 0$ and $H^+(\phi) = 0$ are replaced by

$$\begin{aligned} &H^-(-\phi) - \Delta_1 = 0 \quad \text{at } x = 0, \\ &H^+(\phi) - \Delta_N = 0 \quad \text{at } x = 1. \end{aligned} \tag{10}$$

Provided that $\Delta_1$ and $\Delta_N$ are not too large, Eqs. (10) have solutions $\overline{\phi}_L$, $\overline{\phi}_R$ satisfying the stability conditions $(H^-)'(-\overline{\phi}_L) > 0$, $(H^+)'(\overline{\phi}_R) > 0$. If $H^+ \equiv H^-$ and $\Delta_1 = \Delta_N$, the solution for large $N$ is qualitatively like that of (7) with (9) as boundary conditions, i.e. $\phi_j \approx \overline{\phi}_L$ for the left half of the chain, and $\phi_j \approx \overline{\phi}_R$ for the right half of the chain, with a boundary layer in between [3,23].

### 4.2. Gradients in frequency and random frequencies

For phase oscillators, gradients in frequency that are not too large lead to waves with non-constant speed [5,24]. Though analyses with more random frequencies have not been done, pairs of oscillators having different frequencies cannot lock without phase differences [2,5,24,25].

By contrast, the arguments of Sections 2 and 3 show that for a sufficiently small gradient in times along the left-hand or right-hand branches, or small pairwise differences among successive oscillators, synchrony of jumps can be maintained for chains of relaxation oscillators. This is illustrated in Fig. 13. The figure shows the behavior of a chain of 20 oscillators with a frequency gradient of 50% over the chain. Note that the 50% gradient in frequency can be overcome by the FTM interactions.

*Remark.* The FTM interactions can be provoked by a stimulus that sharpens the synaptic gating function as in Fig. 12. It is also possible for a stimulus to act on a chain of oscillators by directly changing the frequency of the uncoupled oscillators. This happens for example, if the stimulus is modeled (in Morris–Lecar oscillators) by addition of current. With enough added current, the frequencies of the oscillators "saturate" and the gradient disappears (G.B. Ermentrout, personal communication; Somers, unpublished observation). See Ref. [26] for an example in which there is a gradient of frequencies of the uncoupled oscillators. In the absence of a stimulus, there is a travelling wave of activity, which switches quickly to approximate synchrony upon introduction of a stimulus.

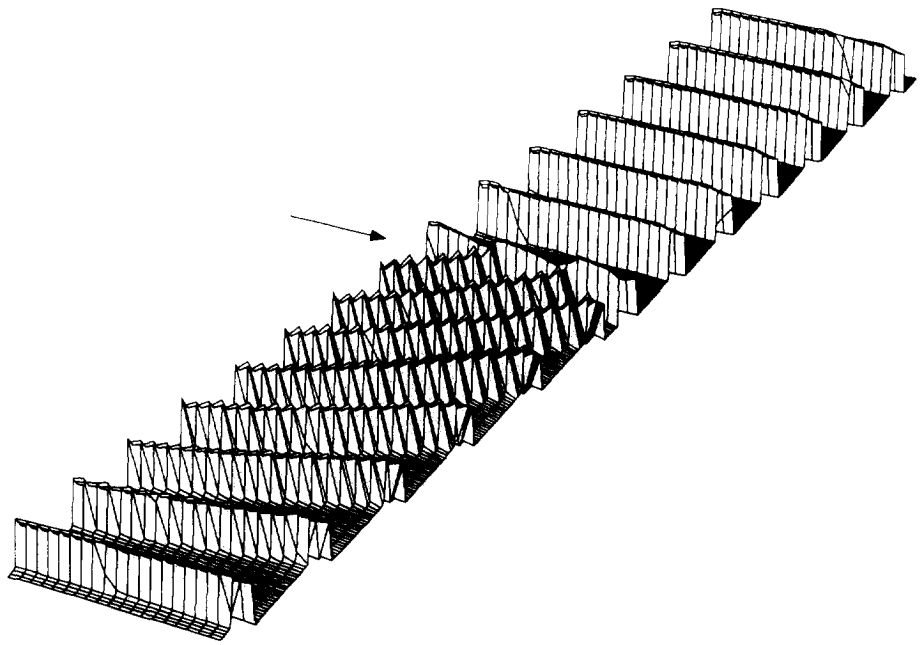

Fig. 13. FTM compensation for a frequency gradient. A chain of 20 relaxation oscillators with a 50% gradient in natural frequencies ($\epsilon = 0.001$ to $\epsilon = 0.0015$) is started with identical initial conditions and zero coupling. Travelling waves propagate across the chain with increasing phase lags. Onset of FTM coupling ($\alpha = 0.2$) (arrow) rapidly synchronizes the chain.

## 5. Fractured synchrony and fractured waves

We now turn to another distinction between chains of phase oscillators and chains of relaxation oscillators. This distinction holds in the context of oscillators that are pairwise capable of displaying stable in-phase and antiphase solutions. For example, a pair of phase oscillators satisfying (2.1) with $\omega_1 = \omega_2 \equiv \omega$ and $H_1 = H_2 \equiv H$ has this property if

$$H(\phi) = A\sin(\phi) + B\sin(2\phi) + C\cos(\phi), \quad (11)$$

with $B \geq A/2 > 0$. Relaxation oscillators coupled through FTM can also exhibit such bistability if the times along the left and right branches are sufficiently different [9].

*Rings* of identical oscillators have synchrony as one solution, and this is stable for phase oscillators if $H'(0) > 0$ and for relaxation oscillators when Hypothesis C is satisfied near one or both jumps. There are also other possible stable solutions, including travelling waves [27]. In the solutions we will now discuss, the ring breaks up into a number of domains. For the phase oscillators, the behavior on individual domains is wave-like, with a pair of waves travelling toward or away from the center of the domain. For the relaxation oscillators, the oscillators within each domain are approximately synchronous, with neighboring domains approximately in antiphase. We call this "fractured synchrony" and the behavior for the phase oscillators "fractured waves." Simulations demonstrating these behaviors are displayed in Figs. 14 and 15, respectively; the relaxation equations are given in the Appendix.

We now give a heuristic explanation why fractured synchrony is to be expected in the relaxation case, and not possible (generically) for phase oscillators. The central idea is that the boundary between the domains creates a pair of oscillators whose antiphase interactions would produce a different frequency and/or waveform from the rest of the chain in the absence of the other oscillators. This "defect" acts like a "pacemaker" for the array. The essential difference between the arrays of relaxation oscillators and

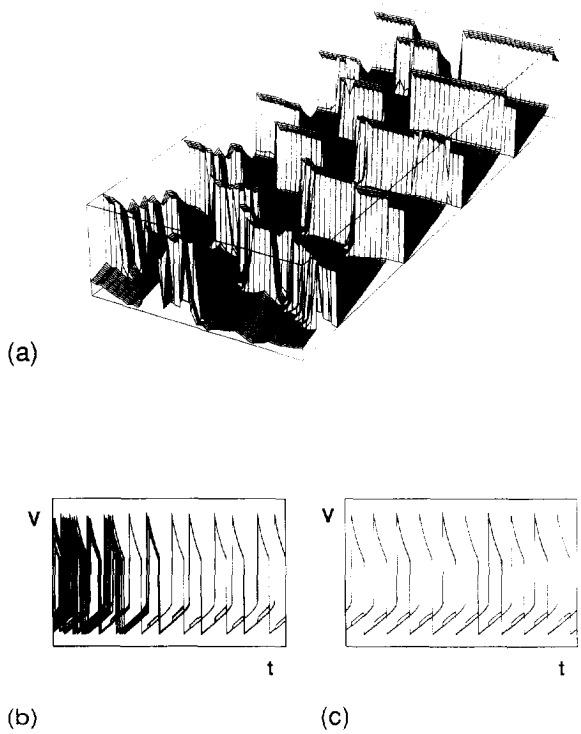


Fig. 14. Fractured Synchrony. A *ring* of 40 uniform relaxation oscillators ($\epsilon = 0.0002$, $\alpha = 0.02$) breaks into two locally synchronized domains of 10 and 30 oscillators each. (a) 3-D view shows formation of contiguous oscillator domains over time. The domain with 30 oscillators wraps around the end positions of the plot. (b) With voltage traces overlaid, tight synchrony can be seen within each of the two domains. Note that the domains are not in precise antiphase. This persisted for as long as the simulation was run (over 100 cycles). (c) Initial conditions corresponding to near antiphase on the same domains yielded trajectories which remain in antiphase for at least 200 cycles. This demonstrates that the phase relationship between domains may depend on the initial conditions the of array.

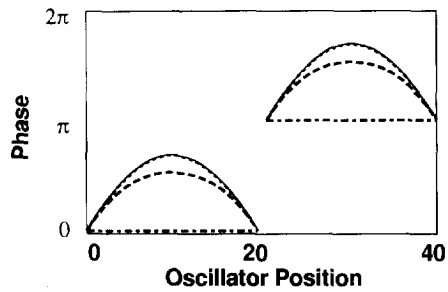


Fig. 15. Fractured waves. A ring of 40 uniform phase oscillators is started as two antiphase domains, each composed of 20 locally synchronous oscillators (flat dot-dash line). For equal sized domains, domain borders remain antiphase and a stable bi-directional travelling wave quickly forms within each domain. Successive curves show relative phases of oscillators after 0, 2, 10, and 100 (solid line) cycles. Degree of bowing increases with domain size. Unlike the relaxation oscillators, here unequal domain sizes lead to changing phase relationships between domain borders (in much less than 100 cycles). In our simulations this led to synchrony or free running phase relationships. ($A = 1.0$, $B = 0.75$, $C = 0.5$).

the phase-difference coupled oscillators is then seen to be in their responses to these defects. In particular, phase-difference coupled oscillators transmit the effects of the pacemaker, while relaxation oscillators localize the effects.

We start with the circle of relaxation oscillators with two domains of oscillators initially in antiphase. To understand the behavior within a domain, consider an equivalent length chain of oscillators, with identical oscillators in the interior, and the end oscillators replaced by ones that have the same times along the left-hand branch and right-hand branch as the antiphase pair. The behavior of the chain depends on the LCI's for the interior and end oscillators as discussed in Section 4.1. If the LCI of the end oscillator is not so different from the LCI of the interior ones, the resulting behavior of the equivalent chain is synchrony, as seen in the domains of Fig. 14. Thus, the effect of the antiphase pair is localized. Simulations show that this is true, independent of the relative domain sizes.

We now turn to phase-difference coupled oscillators and again consider two equal domains of oscillators initially synchronous on each domain, with the domains in antiphase. By symmetry, the lag between the neighboring end oscillators of the domains remains at $\pi$ for all time. Thus, the behavior on a domain is the same as that of a chain whose end oscillators have the same frequency as an antiphase pair. For a phase oscillator with $H$ given by (11), an antiphase solution for two identical oscillators with frequency $\omega$ must satisfy $\theta_j' = \omega + H(\theta_j - \theta_i) = \omega + H(\pi)$. Thus the solution has frequency $\omega + H(\pi) = \omega - C$. $H'(\pi) = -A + 2B > 0$, so this solution is stable. For large $N$, the theory of [5] predicts phase lags $\phi_j \approx \overline{\phi}_L$ for the left half of the chain, $\phi_j \approx \overline{\phi}_R$ for the right half of the chain, with a boundary layer in between, where $\overline{\phi}_L$ (resp. $\overline{\phi}_R$) satisfy

$$H(-\overline{\phi}_L) + C = 0, \quad H(\overline{\phi}_R) + C = 0. \tag{12}$$

Since $\phi_R = -\phi_L$, this argument shows that *if* the oscillators at the domain boundaries are constrained to stay in antiphase, then the behavior on each domain is that of a pair of waves tending toward or away from the domain center. This is shown in Fig. 15. The argument rules out fractured synchrony provided that the conditions $\phi_L \neq 0 \neq \phi_R$ are satisfied. If the domains are not of equal size, the lag between the domains does not remain at $\pi$, and the domains eventually dissolve. In either case fractured synchrony does not occur.

*Remark.* It was shown by Abbott [28] that a network of relaxation oscillators is capable of encoding patterns of "on" and "off" that can be "learned" like static patterns of a Hopfield network. Attempts by Abbott and Kopell to numerically reproduce that effect with phase-difference coupled oscillators did not succeed (unpublished). The work in this paper shows why relaxation oscillators can more robustly encode domains of synchronous/antiphase behavior.

## Acknowledgements

We wish to thank L. Abbott for conversations about the differences between phase and relaxation oscillators.

## Appendix

The Morris–Lecar system [14] is an example of voltage-gated conductance equations. These equations are used as a simplified description of an action potential or of the envelope of a burst of action potentials [29]. The equations for a single oscillator are

$$dv/dt = -g_{Ca} m_\infty(v)(v-1) - g_K\, w(v-v_k) - g_L(v-v_L) + I_{\text{ext}}, \tag{13}$$

$$dw/dt = \epsilon[w_\infty(v) - w]/\tau_w(v), \tag{14}$$

where

$$m_\infty(v) = 0.5[1 + \tanh\{(v-v_1)/v_2\}],$$

$$w_\infty(v) = 0.5[1 + \tanh\{(v-v_3)/v_4\}],$$

$$\tau_w(v) = 1/\cosh\{(v-v_3)/(v_5)\}.$$

The nullclines for these equations and the singular limit cycle, are drawn in Fig. 1. The parameter values used throughout the simulations were $v_1 = -0.01$, $v_2 = 0.15$, $v_3 = 0.1$, $v_4 = 0.145$, $v_5 = 0.29$, $g_{CA} = 1.0$, $g_L = 0.5$, $g_K = 2.0$, $v_L = -0.4$, $v_K = -0.7$, $I = 0.1$. The values of $\epsilon$ are contained in the figure captions. The coupling between a pair of such oscillators is given, as described in Section 2, by adding the term

$$-\alpha g_{Ca} n_\infty(\hat{v})(v-1), \tag{15}$$

where

$$n_\infty(v) = 0.5[1 + \tanh\{(v-v_6)/v_7\}],$$

to (13). Here $\hat{v}$ denotes the voltage of the other oscillator and $\alpha$ represents the coupling strength. $\alpha$ ranged between 0.0 and 0.5 as stated in the figure captions. The parameter values $v_6 = 0.05$, $v_7 = 0.15$ were used, except where noted in the figure captions. For a linear array, there were two such coupling terms, corresponding to the voltages of the two nearest neighbors.

## References

[1] D. Somers and N. Kopell, Biol. Cybern. 68 (1993) 393.
[2] N. Kopell, in: Neural Control of Rhythmic Movements in Vertebrates, A.H. Cohen, S. Rossignol and S. Grillner, eds. (Wiley, New York, 1988) p. 369.
[3] J.D. Murray, Mathematical Biology (Springer, New York, 1989).
[4] J. Guckenheimer and P.J. Holmes, Nonlinear Oscillations, Dynamical Systems, and Bifurcations of Vector Fields (Springer, New York, 1983).
[5] N. Kopell and G.B. Ermentrout, Commun. Pure Appl. Math. 39 (1986) 623.
[6] G. Schöner and J.A.S. Kelso, Biol. Cybern. 58 (1988) 81.
[7] D. Hansel, G. Mato and C. Meunier, Europhys. Lett. 23 (1993) 367.
[8] R.H. Rand and P.J. Holmes, Int. J. Nonlinear Mech. 15 (1980) 387.
[9] N. Kopell and D. Somers, J. Math. Biol. 33 (1995) 261.
[10] J. Bélair and P.J. Holmes, Quart. Appl. Math. 42 (1984) 193.
[11] T. Nordhaus, Echo-cycles in coupled FitzHugh–Nagumo equations, Ph.D. Thesis, University of Utah (1988).
[12] D.W. Storti and R.H. Rand, SIAM J. Appl. Math. 46 (1986) 56.
[13] A.L. Hodgkin and A.F. Huxley, J. Physiol. (London) 117 (1952) 500.

[14] C. Morris and H. Lecar, Biophys. J. 35 (1981) 193.
[15] S.A. Ellias and S. Grossberg, Biol. Cybern. 20 (1975) 69.
[16] H.R. Wilson and J.D. Cowan, Biophys. J. 12 (1972) 1.
[17] DeL. Wang and D. Terman, IEEE Trans. Neural Networks 6 (1995) 283.
[18] P. Pinsky, SIAM J. Appl. Math 55 (1995) 220.
[19] N. Kopell, G.B. Ermentrout and T.F. Williams, SIAM J. Appl. Math 51 (1991) 1397.
[20] R. Harris-Warrick and R. Flamm, J. Neurosci. 7 (1987) 2113.
[21] K. Fox, H. Sato and N. Daw, J. Neurophys. 64 (1990) 1413.
[22] S. Nelson and M. Sur, Curr. Opin. Neurobiol. 2 (1992) 484.
[23] T. Matshushima and S. Grillner, Neuro Report 1 (1990) 97.
[24] A.H. Cohen, P.J. Holmes and R.H. Rand, J. Math. Biol. 13 (1982) 345.
[25] D.M. Kammen, P.J. Holmes and C. Koch, in: Models of Brain Functions, R.M.J. Cotterill, ed. (Cambridge Univ. Press, Cambridge, 1989) p. 273.
[26] D. Kleinfeld, K.R. Delaney, M.S. Fee, J.A. Flores, D.W. Tank and A. Gelperin, J. Neurophysiol. 72 (1994) 1402.
[27] G.B. Ermentrout, J. Math. Biol. 23 (1985) 55.
[28] L. Abbott, J. Phys. A 23 (1990) 3835.
[29] J. Rinzel and G.B. Ermentrout, in: Methods in Neuronal Modeling, C. Koch and I. Segev, eds. (MIT, Cambridge, MA, 1989) p. 135.